Insulator interface effects in sputter-deposited NbN/MgO/NbN (superconductor–insulator–superconductor) tunnel junctions

S. Thakoor and H. G. Leduc
Jet Propulsion Laboratory, California Institute of Technology, Pasadena, California 91109

J. A. Stern
California Institute of Technology, Pasadena, California 91125

A. P. Thakoor and S. K. Khanna
Jet Propulsion Laboratory, California Institute of Technology, Pasadena, California 91109

(Received 5 November 1986; accepted 22 December 1986)

All refractory, NbN/MgO/NbN (superconductor–insulator–superconductor) tunnel junctions have been fabricated by *in situ* sputter deposition. The influence of MgO thickness (0.8–6.0 nm) deposited under different sputtering ambients at various deposition rates on current–voltage (I–V) characteristics of small-area ($30\times30\,\mu$m) tunnel junctions is studied. The NbN/MgO/NbN trilayer is deposited *in situ* by dc reactive magnetron (NbN), and rf magnetron (MgO) sputtering, followed by thermal evaporation of a protective Au cap. Subsequent photolithography, reactive ion etching, planarization, and top contact (Pb/Ag) deposition completes the junction structure. Normal resistance of the junctions with MgO deposited in Ar or Ar and N_2 mixture shows good exponential dependence on the MgO thickness indicating formation of a pin-hole-free uniform barrier layer. Further, a postdeposition *in situ* oxygen plasma treatment of the MgO layer increases the junction resistance sharply, and reduces the subgap leakage. A possible enrichment of the MgO layer stoichiometry by the oxygen plasma treatment is suggested. A sumgap as high as 5.7 mV is observed for such a junction.

I. INTRODUCTION

All refractory, high T_c material based, superconductor–insulator–superconductor (SIS) tunnel junctions (e.g., NbN/MgO/NbN) are ideally suited for use as quantum mixers in submillimeter wave heterodyne receivers.[1,2] The robustness of all such refractory devices makes them extremely stable for repeated thermal cycling and long-term use. For an SIS tunnel junction to be used as a sensitive low-noise mixer for high frequencies (up to 1500 GHz), it should have a high superconducting sumgap ($\Delta_\Sigma \sim 6$ mV), a high-subgap leakage resistance R_{sg} computed at one-half the sumgap value (~ 3 mV), and a sharp nonlinearity, i.e., a small ΔV, the width of the quasiparticle tunneling onset. The quality of the junction is usually expressed as the quality factor $V_m = I_c R_{sg}$, where I_c is the Josephson critical current.

Recently[3–5] sumgap values in excess of 5 mV have been demonstrated for NbN/MgO/NbN junctions proving the advantage of using a thermodynamically stable artificial barrier like MgO over the native oxide barrier. The native oxide barrier grown on base NbN is known to cause reduction of the energy gap of the counterelectrode through a reaction of NbN with oxygen atoms from the barrier (Nb_2O_5) at the interface, a critical region in the junction. In addition to the overall quality of the bulk of NbN electrodes, it is crucial to have the high T_c, $B1$ phase of NbN at the NbN/MgO interfaces. Further, the interfaces should also be physically smooth and contamination free. To achieve this, *in situ* deposition of the junction trilayer, NbN/MgO/NbN is the usual choice. Reactive dc magnetron sputtering has been successfully used[2–6] to deposit the NbN base and counterelectrodes. A variety of techniques[1,3,7] have been explored to obtain uniform, homogeneous, mechanically and chemically stable, thin MgO layers. Thermal oxidation or ion beam oxidation of thin magnesium overlayers has been used by Talvacchio *et al.*[7]; the resulting junctions were quite leaky, probably due to the tendency of unoxidized Mg to diffuse into the base electrode. It has been further suggested[8,9] that polyepitaxy or single-crystal epitaxy (during the junction trilayer deposition) may be useful in realizing the full sumgap in an all NbN junction. Normally high substrate temperature and/or single-crystal substrates are used to induce such epitaxial growth. In a recent study[1] in our laboratory, an anomalous dependence of the tunneling resistance on barrier thickness is observed for junctions with electron beam (e-beam) deposited MgO barriers. The Stranski–Krastinov mechanism for epitaxial growth has been proposed to explain this data. In this growth mode, the first monolayer of MgO grows extremely coherently, essentially to minimize the free energy at the surface. However, later growth of MgO occurs by nucleation, resulting in a barrier of somewhat nonuniform thickness. Tunneling through the thinner barrier regions then dominates the junction's I–V characteristics. Alternatively, rf sputtering of MgO has been successfully used by Shoji *et al.*[3–6] yielding high-quality junctions ($\Delta_\Sigma = 5.4$ mV) with barrier thickness as low as 0.5 nm without any special parameters to induce MgO epitaxy. Moreover, rf sputtering of MgO does not require ultrahigh vaccum; such an "all-sputter-deposition" sequence thus allows quick changes between NbN deposition and MgO deposition by simple repositioning of the substrates with respect to the sputter targets. This may have some effect in minimizing contamination of the junction interfaces from the chamber ambient. Futhermore, vapor flux in sputter deposition

 0734-2101/87/041721-05$01.00

reaches the substrate over a wide range of incidence angles due to the multiple scattering and small mean free path in the sputtering ambient. This is in contrast with the line of sight deposition by a technique such as e-beam evaporation in UHV. Sputter deposition is therefore expected to yield a better coverage and thickness uniformity over the substrate, which may be further enhanced by substrate rotation.

In this paper, we report on the influence of deposition conditions on the performance of sputter deposited NbN/MgO/NbN tunnel junctions. MgO films are deposited with substrate rotation in ambients of high-purity Ar and Ar + N_2 mixture. The junction resistance as a function of effective MgO thickness ranging from 0.8 to 6.0 nm is studied.

II. EXPERIMENTAL DETAILS

A. Deposition

A four-layer structure composed of a dc reactively sputtered NbN base (~360 nm), rf magnetron sputtered MgO barrier (~0.8 to 6.0 nm), a counter NbN electrode (~120 nm), and finally a thermally evaporated protective gold coating (~50 nm) was deposited *in situ* on sapphire substrates. An ultrahigh-vacuum system described elsewhere[6] was modified to include an rf magnetron sputtering gun for a 2-in.-diam MgO target, in addition to a dc magnetron sputtering gun for a 2-in.-diam Nb target, a substrate holder which can be rotated axially, and a source for thermal evaporation of gold. A bottom-up deposition geometry was used with the substrates ~6.25 cm away from the Nb target and ~10 cm away from the MgO target. No intentional substrate heating or cooling was utilized. The superconducting NbN films for the base as well as the counterelectrode were deposited by dc reactive magnetron sputtering of the Nb target (99.99% pure) in a mixture of Ar and N_2 gases (99.999% pure). The nitrogen consumption injection characteristics for the reactive sputter deposition of NbN established earlier[6] were used as guidelines for fine tuning the deposition parameters to yield high T_c NbN in the modified configuration of the system. Typical characteristics of the NbN films utilized for the junction fabrication are as follows: Superconducting transition temperature T_c: ~16 K, transition width: 0.2 K, resistivity: 175 $\mu\Omega$ cm, and resistance ratio $R_{300\ K}/R_{29\ K}$: 0.95. The MgO barrier layer was deposited by rf magnetron sputtering in pure argon (~13 mTorr). However, barrier layers for some junctions were deposited by sputtering of MgO in a mixture of Ar (~13 mTorr) and N_2 (~3.6 mTorr), the same gas composition as selected for a deposition of high-T_c NbN films. In addition to a study of the effect of nitrogen presence during sputtering of MgO on its film quality, such a sequence also reduced the time between the deposition of the subsequent layers since the sputtering ambient did not require a readjustment for each layer.

To obtain a uniform coverage of MgO film over the NbN base layer, and a better control over the film thickness/deposition rate, particularly for thin (<2.5 nm) MgO layers, substrate rotation (~30 rpm) was used. Thicker (2.5–6.0 nm) MgO films, however, were obtained by deposition on stationary substrates. The MgO thickness was varied by varying the product of the power applied to the target and the total deposition time. At 400 W of power, a direct deposition rate of ~2 nm/min was obtained, as measured on a precalibrated quartz-crystal oscillator, whereas, with rotation, the effective deposition rate became ~0.4 nm/min. The values of barrier thickness so controlled are accurate to ~0.015 nm. The MgO thickness was systematically varied in the range of ~0.8 to 6.0 nm. The effect of an additional post-MgO-deposition, *in situ* plasma oxidation treatment (in 75 mT pressure of 99.999% pure oxygen) at 500 V for 3 min was studied in some junctions particularly with thin (≤2.5 nm) MgO layers.

B. Junction patterning

The gold cap over the junction trilayer prevented oxidation of the NbN counterelectrode top surface on exposure of the deposited quadlayer to atmosphere. The fabrication steps are shown schematically in Fig. 1. Standard photolithography (photoresist AZ4330), was used to mask the area of the junction (30×30 μm). Selective reactive ion etching of the top gold layer by $CClF_3$, followed by etching through the NbN counterelectrode with CF_4, defined the junction area in the form of a mesa structure. Next the base electrode was electrically isolated and the mesa structure was planarized by thermally evaporating an SiO layer (~300–500 nm).

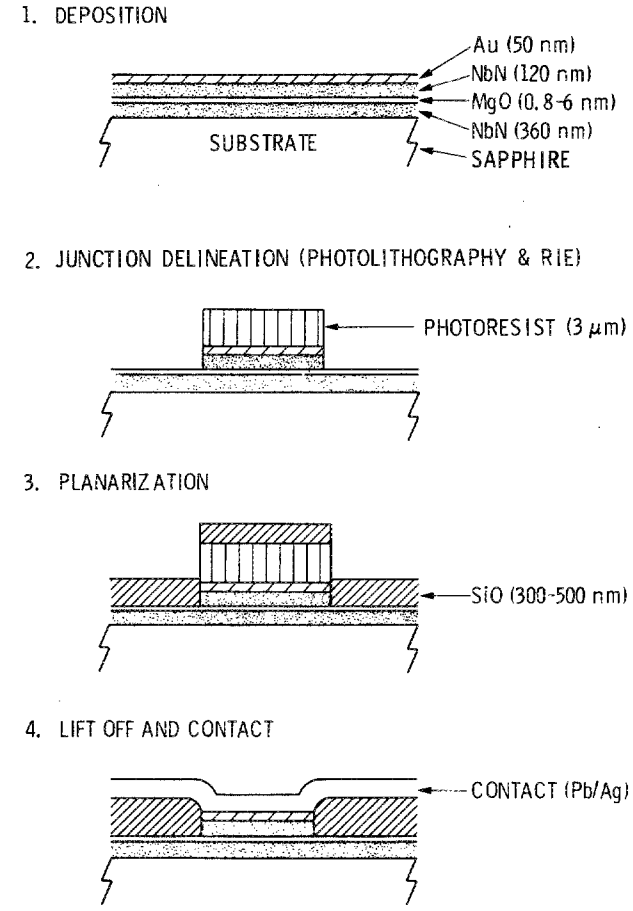

FIG. 1. Schematic representation of the junction patterning process: (a) deposition, (b) junction delineation (photolithography and RIE), (c) planarization, and (d) liftoff and contact.

Finally the photoresist mask is lifted off and a contact electrode (Pb/Ag) is thermally evaporated onto the gold cap to complete the structure. In essence, other than the gold etch step the patterning process is similar to that used by Shoji *et al.*[10] The current–voltage (I–V) characteristics of these SIS junctions were measured at 4.2 K to study their electron tunneling properties and thereby the junction quality.

III. RESULTS AND DISCUSSION

The deposition rate of MgO was found to be the most important parameter in obtaining good junctions. For lower sputtering power (<250 W) the junction yield was very poor. Junction shorts indicated that the MgO layer mostly suffered from pin holes. A 400-W power level for deposition was found to be optimum and was used for the following study. Figure 2 shows a typical I–V characteristic of a junction with $\sim$1.0-nm-thick MgO. It has a sumgap of $\sim$4.8 mV, normal resistance R_N (at 8 mV) $\sim 1\ \Omega$, and the Josephson current I_c $\sim$2.3 mA ($\sim$2/3 of the theoretical value as calculated using the Ambegaokar–Baratoff relation[11]).

The presence of N_2 in the sputtering ambient during the deposition of MgO had little effect on its deposition rate as well as the barrier quality. Junctions prepared with MgO deposited with or without N_2 showed comparable junction quality. This suggests that N_2 does not interfere, physically or chemically, with the growth kinetics of MgO; and that the reduced time gap between the deposition of successive layers of the tri-structure, expected to reduce the "interface-contamination" effects, had undetectable effect on the overall interface quality. Sumgaps of the junctions made with or without N_2 during the MgO deposition, ranged mostly from $\sim$4.5 to $\sim$5.2 mV, however, a sumgap of as high as $\sim$5.7 mV (Fig. 3) has been observed. Although large sumgap values are achieved in these junctions, the large ΔV ($\sim$1 mV) should be primarily attributed to the spatial variation in the NbN quality over the active area ($\sim 900\ \mu m^2$) at the junction interface.

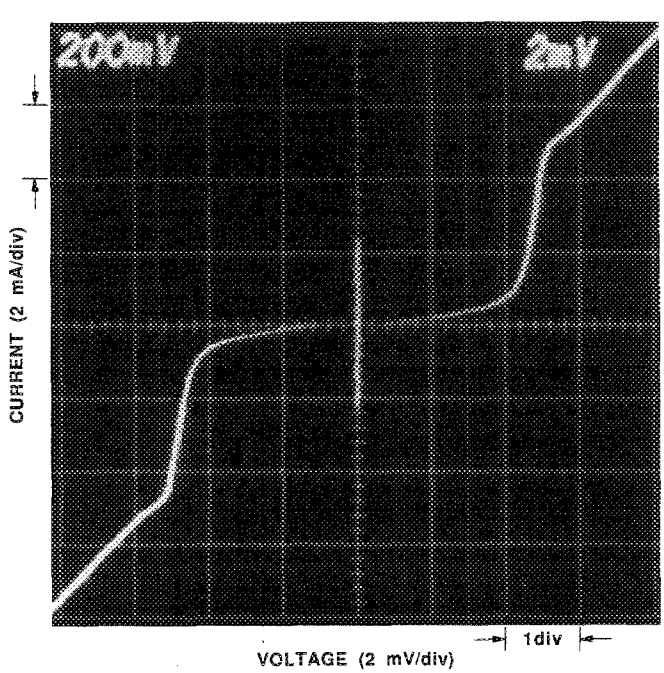

FIG. 2. Typical current–voltage (I–V) characteristics for a junction with MgO thickness $\sim$1.0 nm.

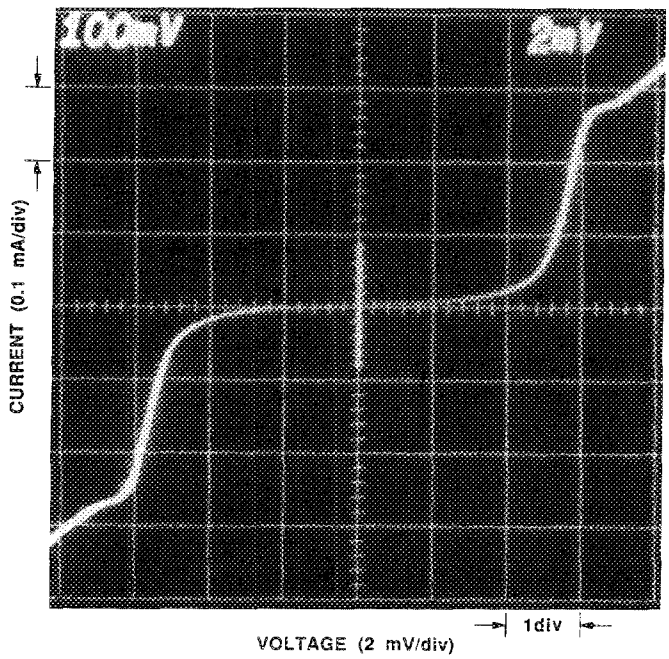

FIG. 3. Current–voltage (I–V) characteristics of a junction with as-deposited MgO thickness $\sim$1.8 nm, followed by plasma oxidation treatment, exhibiting a sumgap $\Delta_\Sigma \sim 5.7$ mV and quality factor $V_m \sim 27$ mV.

Figure 4 shows a plot of the normal resistance (R_N at 8 mV) of junctions of varying MgO thickness, deposited with or without N_2, as well as some with a post-plasma-oxidation treatment. Clearly, the junctions made with MgO (Ar + N_2) are indistinguishable from those with MgO (Ar). The linear dependence of log R_N on MgO thickness, down to $\sim$0.8 nm, indicates formation of a coherent, continuous layer of MgO in these junctions. This is unlike the MgO

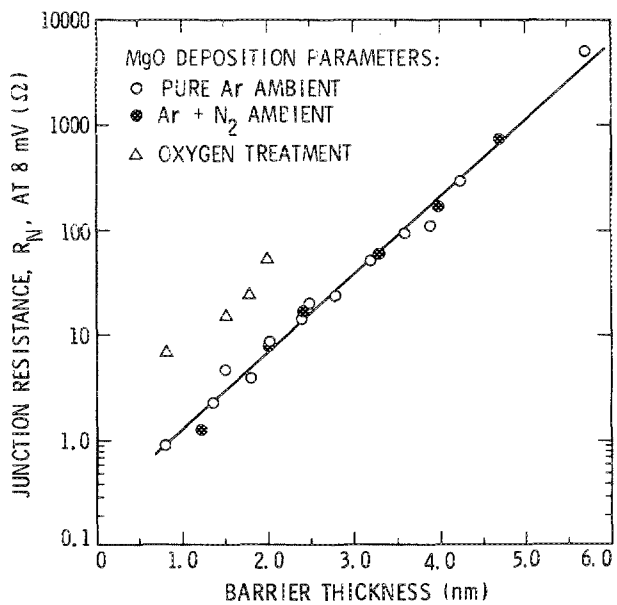

FIG. 4. Junction resistance R_n (at 8 mV) as a function of as-deposited MgO thickness.

barrier recently grown by e-beam evaporation[1] in our laboratory, where the growth is believed to follow the Stranski–Krastinov model. The growth of coherent MgO with uniform thickness in the present case should be primarily attributed to the wide range of incidence angles due to the multiple scattering of vapor flux in sputtering, further enhanced by a fast substrate rotation.

If, however, the MgO barrier layer is truly uniform and coherent, then the rather low subgap resistance ($R_{sg} \sim 7.5\ \Omega$ at 3 mV, Fig. 2) suggests the possibility of an inherently leaky MgO. It is known[12] that MgO films prepared by physical vapor deposition can be off stoichiometric as MgO can decompose in the vapor phase. On the other hand, smooth, superstoichiometric MgO_x films have been deposited by ion beam sputtering[13] of Mg (using Ar ions in a reactive oxygen ambient) with improved mechanical and dielectric properties. It is also observed that surface quality of MgO films could be substantially improved at high temperatures by an "oxygen treatment."[14]

Deposition of MgO in a mixture of Ar and O_2 was not desirable in the present case, since it could cause a degradation of the surface of base NbN by its partial oxidation. As an alternative, the NbN base was first "sealed" with MgO layer deposited in pure Ar and then it was subjected immediately afterwards to an *in situ* plasma oxidation treatment. It has been recently reported[15] that "wet" plasma oxidation of thin Mg films had better success than a dry plasma oxidation treatment in obtaining good-quality thin, continuous MgO barrier layers for Mg–MgO–Pb tunnel junctions. In the present case, however, water vapor was not intentionally added during the oxidation treatment. Figures 5(a) and 5(b) show I–V characteristics of two junctions, with 0.8-nm-thick MgO, without and with oxygen plasma treatment, respectively. The parameters for the two junctions are $\Delta_\Sigma = 5.1$ mV, 5.2 mV, $R_n = 0.95\ \Omega$, 6.9 Ω; $R_{sg} = 5\ \Omega$, 75 Ω; and quality factor $V_m = 12$, 25, respectively. A substantial improvement in the subgap leakage resistance is clearly evident. The normal resistance (R_N at 8 mV) for a set of junctions with oxygen treated MgO is plotted in Fig. 4, for comparison. The increased normal resistance for a given thickness of MgO is probably an indication of significantly changed MgO. If the observed R_N value of the junction in Fig. 5(b) is attributed primarily to the change in physical thickness of as-deposited MgO, it should have changed from ~1 to ~2 nm. Such a change in MgO film thickness is unexpected. On the other hand, this treatment may have caused an oxygen enrichment of the as-deposited MgO giving rise to a superstoichiometric phase as obtained by Hebard *et al.*,[13] with improved dielectric properties. Thus, the observed change in resistance is possibly a cumulative effect of a significant change in the dielectric properties accompanied with an associated minor change in the physical thickness of MgO. Although the junction sumgap and oxygen treatment of MgO were not directly correlated, the high sumgap ($\Delta_\Sigma \sim 5.7$ mV, Fig. 3) was realized in a junction with oxygen treatment MgO.

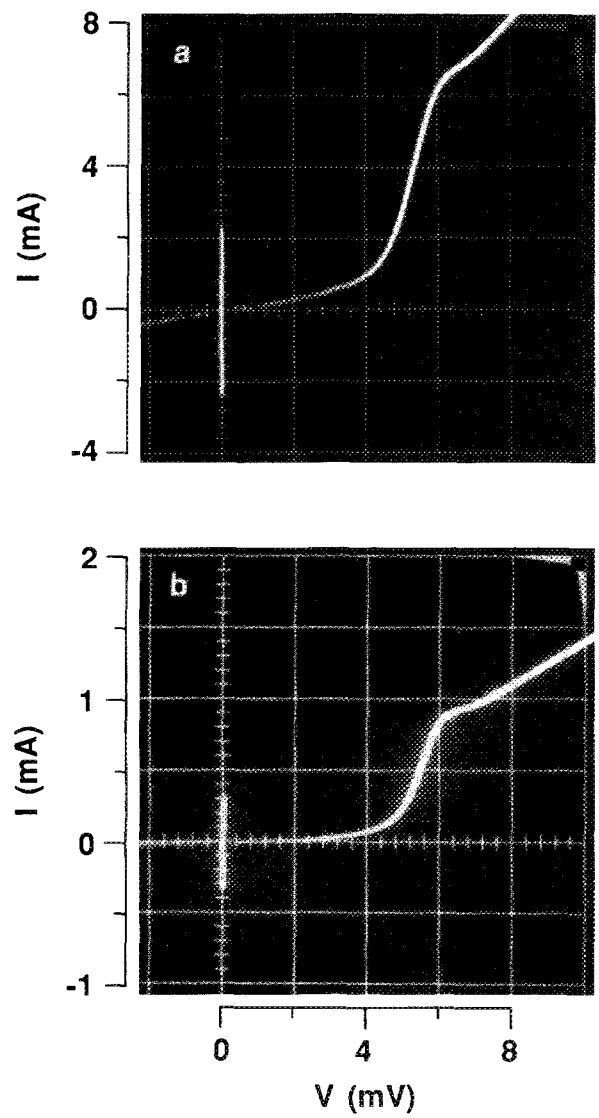

FIG. 5. Current–voltage (I–V) characteristics of junctions, (a) without and (b) with post-MgO-deposition, *in situ* plasma oxidation treatment.

IV. CONCLUSIONS

All refractory, sputter-deposited NbN/MgO/NbN junctions with sumgap Δ_Σ as high as 5.7 mV, and quality factor $V_m \sim 27$ have been fabricated. In these junctions the formation of coherent, pin-hole-free MgO barrier layers, as thin as 0.8 nm, is confirmed by the exponential dependence of R_N on MgO thickness. Junctions made from trilayers with MgO deposited in pure argon or argon and nitrogen mixture showed comparable junction quality. An *in situ*, post-MgO-deposition, oxygen treatment improved the subgap leakage considerably, thus improving the quality of the junction. This improvement is attributed to the oxygen enrichment of the MgO, enhancing its stoichiometry and thereby its dielectric properties.

ACKNOWLEDGMENTS

This work was carried out by the Jet Propulsion Laboratory, California Institute of Technology, and was supported by the National Aeronautics and Space Administration (NASA) and Strategic Defense Initiative Organization (SDIO) through an interagency agreement with NASA. We

benefited greatly from discussions with Dr. John Lambe and Professor Tom Phillips.

[1]H. G. Leduc, J.A. Stern, S. Thakoor, and S. K. Khanna, Applied Superconductivity Conference, 1986.
[2]S. Thakoor, H. G. Leduc, A. P. Thakoor, J. Lambe, and S. K. Khanna, J. Vac. Sci. Technol. A **4**, 528 (1986).
[3]A. Shoji, M. Aoyago, S. Kosaka, F. Shinoki, and H. Hayakawa, Appl. Phys. Lett. **46**, 1098 (1985).
[4]T. Yamashita, K. Hamasaki, and T. Komata, in *Advances in Cryogenic Engineering-Materials*, edited by A. F. Clark and R. P. Reed (Plenum, New York, 1986), Vol. 32, pp. 617–626.
[5]A. Shoji, M. Aoyagi, S. Kosaka, and F. Shinoki, Applied Superconductivity Conference, 1986.
[6]S. Thakoor, J. L. Lamb, A. P. Thakoor, and S. K. Khanna, J. Appl. Phys. **58**, 4643 (1985).
[7]J. Talvacchio, J. R. Gavaler, A. I. Braginski, and M. A. Janocko, J. Appl. Phys. **58**, 4638 (1985).
[8]J. Talvacchio and A. I. Braginski, Applied Superconductivity Conference, 1986.
[9]G.-I. Oya, M. Koishi, and Y. Sawada, J. Appl. Phys. **60**, 1440 (1986).
[10]A. Shoji, F. Shinoki, S. Kosaka, M. Aoyagi, and H. Hayakawa, Appl. Phys. Lett. **41**, 1097 (1982).
[11]V. Ambegaokar and A. Baratoff, Phys. Rev. Lett. **10**, 485 (1963); **11**, 104(E) (1963).
[12]*Handbook of Thin Film Technology*, edited by L. I. Maissel and R. Glang (McGraw–Hill, New York, 1970), pp. 1–70.
[13]A. F. Hebard, A. T. Fiory, S. Nakahara, and R. H. Eick, Appl. Phys. Lett. **48**, 520 (1986).
[14]R. Dale Moorhead and H. Poppa, Thin Solid Films **58**, 169 (1979).
[15]W. Plesiewicz and J. G. Adler, Phys. Rev. B **34**, 4583 (1986).